Self-Assembly Behavior of Alkylated Isophthalic Acids Revisited: Concentration in Control and Guest Induced Phase Transformation

Kwang-Won Park[1,2], Jinne Adisoejoso[1*], Jan Plas[1], Jongin Hong[2], Klaus Müllen[3], Steven De Feyter[1*]

1. Division of Molecular Imaging and Photonics, Department of Chemistry, KU Leuven, Celestijnenlaan 200 F, 3001 Leuven, Belgium.

2. Department of Chemistry, Laboratory of Nano-material Chemistry, Chung-Ang University, Seoul 156-756, Republic of Korea

3. Max-Planck Institute for Polymer Research, Ackermannweg 10, D-55128, Mainz, Germany.

Key words: phase behavior, host-guest systems, concentration control, scanning tunneling microscopy, self-assembly

Abstract

The engineering of two-dimensional crystals by physisorption-based molecular self-assembly at the liquid-solid interface is a powerful method to functionalize and nanostructure surfaces. Formation of high symmetry networks from low symmetry building blocks is a particularly important target. Alkylated isophthalic acid (ISA) derivatives are early test systems, and it was demonstrated that in order to produce a so-called porous hexagonal packing of plane group *p*6, i.e. a regular array of nanowells, either short alkyl chains or the introduction of bulky groups within the chains were mandatory. After all, the van der Waals interactions between adjacent alkyl chains or alkyl chains and

the surface would dominate the ideal hydrogen bonding between the carboxyl groups and therefore a close packed lamella structure (plane group *p*2) was uniquely observed. In this contribution, we show two versatile approaches to circumvent this problem, which are based on well-known principles: the "concentration in control" and the "guest induced transformation" method. The successful application of these methods makes ISA suitable building blocks to engineer a porous pattern in which the distance between the pores can be tuned with nanometer precision.

Introduction

Surface confined two-dimensional (2D) crystals consisting of molecular building blocks have garnered a broad interest in nanoscience due to their potential applications.[1-4] Traditionally, non-covalent interactions are used to guide the self-assembly process. By using hydrogen bonding[5-8], van der Waals interactions[9-12], metal-ligand coordination[13-15] or a combination thereof as a molecular 'glue', a multitude of architectures have been successfully engineered both in ultra-high vacuum conditions as well as at a liquid-solid interface. Predicting the specific outcome of network formation based on the molecular building blocks remains a challenge as various experimental factors govern the self-assembly process: solute concentration,[10,16-20] temperature[21-25], solvent [26,27] have all been known to influence the 2D crystal formation under ambient conditions.

It has previously been reported that alkylated isophthalic acid derivatives (ISA) show a variety of self-assembly motifs at the liquid/highly oriented pyrolytic graphite (HOPG) interface, where the outcome is determined by changes of the alkyl chains.[28-30] The main driving force for self-assembly was expected to be the intermolecular interaction between carboxylic groups in meta position, which, after dimerization through hydrogen bonding, potentially could yield linear zig-zag or hexameric structures. It turned out however, that ISA derivatives with a simple linear alkyl chain uniquely formed a lamellar

structure in which the intermolecular van der Waals interactions between adjacent interdigitated alkyl chains as well as the interaction between the chains and the underlying graphite dominate the hydrogen bonding. This forces the structure to circumvent ideal hydrogen bond formation. Only by significantly reducing the alkyl chain length and thereby lowering the impact of van der Waals interactions in favor of hydrogen bonding, cyclic hexameric structures were obtained.[29] As an alternative approach, the introduction of bulky groups at the end of the alkyl tails which prevent ideal alkyl chain interdigitation also produced hexameric structures.[28]

In this work, we show two simple approaches to create 2D nanoporous hexameric patterns at the liquid-solid interface using alkylated ISA derivatives without any inherent structural modifications of the building blocks, which are based on two well-known principles: "concentration in control"[16] and "guest-induced transformation"[31].

Results & Discussions

1. Concentration in Control

Three ISA derivatives (5-decyloxy-isophthalic acid (ISA-OC10), 5-tetradecyloxy-isophthalic acid, (ISA-OC14) and 5-octadecyloxy-isophthalic acid (ISA-OC18)) which differ only in the length of the alkyl chains were chosen (scheme 1) and their 2D self-assembly behavior at the liquid-solid interface was explored by scanning tunneling microscopy (STM). These molecular building blocks have two intrinsic recognition sites for non-covalent interactions: the alkyl chains give rise to van der Waals interactions through interdigitation and the carboxylic acid groups form hydrogen bonds. Depending on the solute concentration used, ISA-OC10 as well as –OC14 form a mixture of two distinct polymorphs , linear and porous, upon adsorption at the 1-phenyloctane/HOPG interface, while ISA-

OC18 yields only the linear polymorph (Figure S2,3,4). Figure 1 shows high-resolution STM images of the linear and porous polymorphs formed by ISA-OC14. At relatively high concentration, a lamellar structure is predominantly observed for all three derivatives, similar to what has been reported earlier.[28,29] Within this lamellar structure, the van der Waals interactions clearly dominate the hydrogen bond formation and forces the molecules into a close packed *p2* structure. The aromatic ISA head groups appear as bright circles. Based on the STM contrast it was impossible to determine the exact orientation or nature of the hydrogen bonds between the ISA head groups; but due to their head-to-head orientation (blue line in Figure 1a), dimer formation between the carboxylic acid functionalities can be excluded.[32] It remains uncertain, however, how the ISA headgroups interact, therefore only tentative models are given in Figure 1a and S1. The angle between the lamella axis and the alkyl chains is 90±1° for ISA-OC18, while for ISA-OC14 (α=84±1° and β=86±1°, Figure 1a) and ISA-OC10 (α=78±1° and β=86±1°, Figure S1) two distinct orientations are observed. While for ISA-OC18 all alkyl chains are oriented parallel to one of main symmetry axes of HOPG, only the alkyl chains following the β angle (between lamella axis and the alkyl chains) are parallel to the main symmetry axis of HOPG.[33] This disparity can be understood as follows: relatively shorter alkyl chains give rise to a smaller contribution of van der Waals interactions to the structure formation and the hydrogen bonds are therefore playing a more important role. However; the former still remains the dominant driving force for self-assembly. Bernasek *et al* estimated the energy contributions of hydrogen bond formation and van der Waals interaction in the lamellar structure of ISA-OC10 and ISA-OC18.[29] They confirmed that the share of hydrogen bonds (30-50 kJ/mol for both ISA-OC10 and ISA-OC18) increases as the share of van der Waals interaction decreases with shorter alkyl chains (108-126 kJ/mol for ISA-OC18 to 60-70 kJ/mol for ISA-OC10).

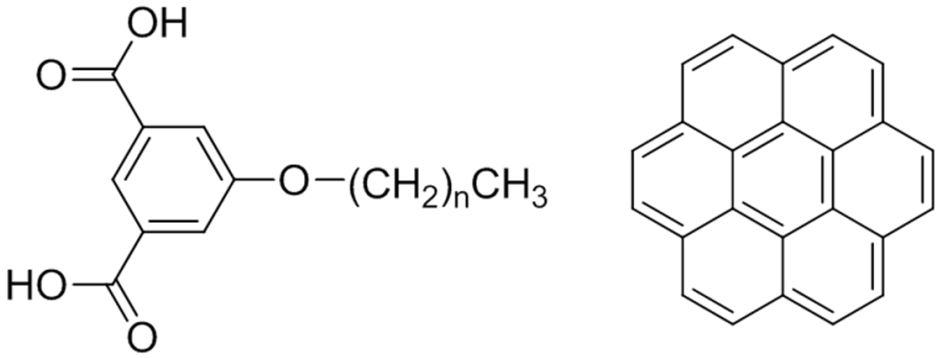

Scheme 1. Molecular structure of ISA-OCn molecules (left): n=9 for ISA-OC10, n=13 for ISA-OC14, n=17 for ISA-OC18. Molecular structure of coronene (right).

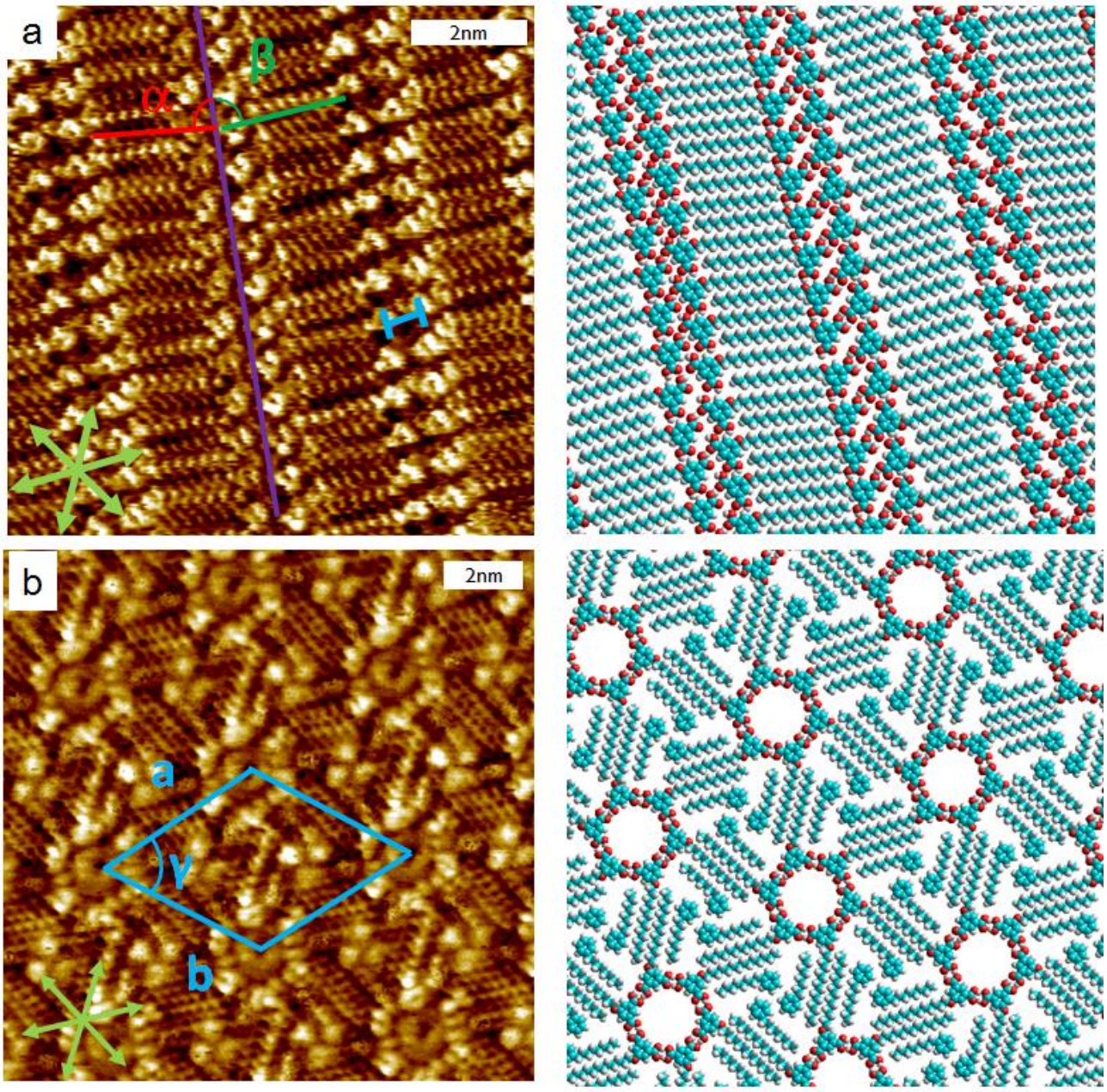

Figure 1. STM images and corresponding tentative molecular models of ISA-OC14 at the 1-phenyloctane / HOPG interface (0.52mM, V_{bias} = 0.55 V, I_{set}= 0.13 nA), showing a) the linear *p2* network (α and β indicate the angle between the alkyl chains and the lamella axis) and b) The hexameric porous *p6* phase (γ = 61 ± 4º, a = 4.00 ± 0.2 nm, b = 4.30 ± 0.1 nm). The blue line indicates the distance between adjacent aromatic parts of ISA molecules. HOPG lattice vectors are indicated in green.

Coexisting with the lamellar structure, ISA-OC10 and ISA-OC14 also form a hexameric porous *p6* structure at higher concentration, which is phase separated from the lamellar network. Lowering the solute concentration leads to the unique formation of this hexameric porous structure for ISA-OC10 and ISA-OC14 (Figure S1 and 1b, respectively), while the lamellar structure of ISA-OC18 seems to be unaffected by solute concentration: it is still uniquely observed. Unlike the lamellar structure, within the hexameric structure the hydrogen bonding is the dominant intermolecular interaction and the system adapts ideal hydrogen bond formation i.e. the dimer formation between adjacent carboxylic acids as observed previously in case of non-alkylated ISA[34] and structurally related trimesic acids[32]. The hydrogen bonded hexagonal pores are in their turn surrounded by six triangular pores, formed by van der Waals mediated alkyl chain interdigitation. After close inspection, it was found that for ISA-OC14 3 phenyloctane solvent molecules reside in the triangular pores, identified by their bright aromatic headgroups.[35] Coadsorption of these solvent molecules compensates for the loss in stability due to the large unoccupied areas in the triangular pores. Within the hexameric structure of ISA-OC10, the triangular pores become too small for solvent coadsorption and appear featureless. This explains why the decrease of the hexameric structure coverage with increasing concentration happens much faster for ISA-OC10 in respect to ISA-OC14. Decreasing the alkyl chain length maintains the hexagonal pore diameter constant (1.13± 0.1 nm), while decreasing the area of the triangular pores or in other words decreasing the distance between adjacent hexagonal pores.

The dependence of the surface coverage of porous polymorph on the concentration of ISA in solution is shown in Figure 2.[36]. As can be seen from the graph, for both ISA-OC10 and ISA-OC14, the porous hexameric structure can be homogenously engineered by using sufficiently low concentration. Surprisingly, even at the lowest concentration probed (0.01 mM) ISA-OC18 still exclusively forms the lamellar network even though the surface coverage becomes sub-monolayer (Figure S4).

The concentration dependency of ISA derivatives is in good agreement with what has been observed earlier with similar molecular building blocks.[16] Traditionally, systems that are sensitive towards concentration consist of building blocks which are able to form two or more polymorphs with different adsorption energy and/or packing density. For ISA-OC10 and ISA-OC14, the packing density of the lamellar structure (1.23 molecules/nm² for ISA-OC10, 0.69 molecules/nm^2 for ISA-OC14) and the hexameric structure (0.48 molecules/nm² for ISA-OC10, 0.33 molecules/nm^2 for ISA-OC14) differs significantly. Therefore at high concentration, the number of molecules exceeds the amount required to cover the surface through hexameric structures and the system reacts by forming the close-packed lamella structure, by using van der Waals forces between alkyl chains as the dominant driving force. However at lower concentration, less molecules are present at the interface and the system will react by forming the low density network and allowing hydrogen-bond formation dictating the structure. Compared to ISA-OC10 and ISA-OC14, the difference in packing density between lamella and hexamers of ISA-OC18 is even larger. However, the energy penalty induced by the uncovered area of the triangular pores is simply too large and therefore, even at sub-monolayer coverage, the formation of lamellae of ISA-OC18 is uniquely observed (Figure S4).

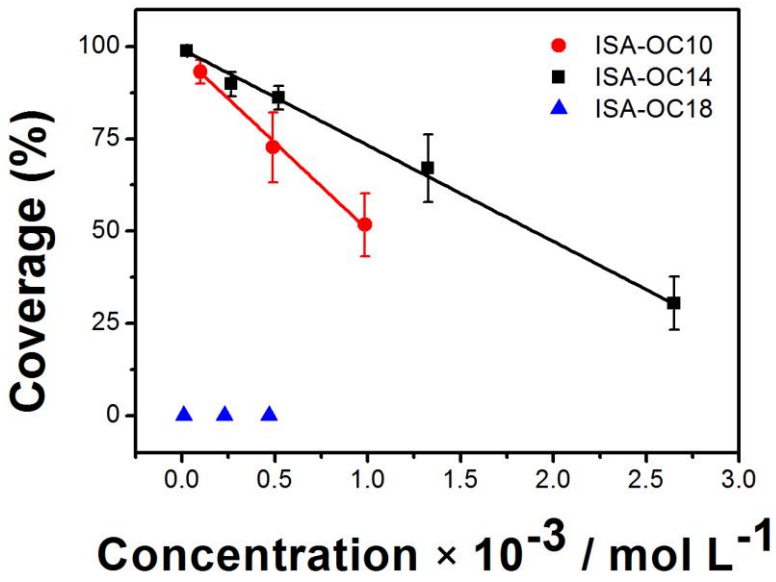

Figure 2. Dependence of the surface coverage of the porous structure on the ISA concentration in solution. For each concentration, typically 10 to 15 large scale images (100 nm × 100nm) were recorded at different locations in order to be statistically relevant (Figure S3)

2. Guest induced transformation

One of the main applications for nanoporous systems is the selective trapping of guest molecules in a spatially resolved manner. Moreover, apart from simple coadsorption, it has been well documented that the addition of guest molecules can overcome the energy loss caused by unoccupied areas and thereby templating the formation of a specific network.[31,37-39] As non-alkylated ISA has been successfully applied to host coronene (COR), COR was chosen as guest for the alkylated ISA host-network.[34]

Upon premixing COR and the alkylated ISA derivatives in a 1:1 molar ratio (COR/ISA-OC10 1mM/0.98mM, COR/ISA-OC14 3mM/2.65mM, COR/ISA-OC18 0.5mM/0.47mM), the hexameric structure is exclusively observed for all the three derivatives (Figure 3a-c). The COR molecules appear as bright circular features within the hexagonal hydrogen-bonded pores of ISA. In the absence of COR, but maintaining the same concentration of the ISA derivatives, the lamellar structure is the dominant polymorph. Therefore, COR not only acts as a guest molecule. Under conditions where ISA forms a lamellar structure, its presence forces the system to transform from a lamellar structure into the hexameric network. After closer inspection, it appears that both for ISA-OC18 and ISA-OC14 (Figure 3b-c), the triangular pores are also accommodating COR molecules. In the case of ISA-OC18, the COR molecules inside the triangular pores appear as fuzzy features, while the COR molecules inside the hexagonal void are well resolved, which can be correlated to the size mismatch between the

triangular void and the adsorption of 1 COR molecule Based on molecular modelling, a COR molecule adsorbed inside the triangular pore has the freedom to rotate and translate and the dynamic nature of COR adsorption into size-mismatched pores has been reported previously.[11] The COR molecules hosted inside the triangular pores of ISA-OC14, however, appear to be well immobilized and even though the triangular pore does not match the hexagonal shape of the COR molecule, the size matching appears to be sufficient to immobilize COR. In contrast, the presence of COR has a more dramatic effect on the hexameric structure of ISA-OC10. Based on molecular modeling, the triangular pore of ISA-OC10 would be too small for the coadsorption of COR. COR addition, however, changes the hexameric patterns such that within a hexamer of ISA-OC10, four out of six alkyl chains are not interdigitated, thus creating additional empty space for the adsorption of COR. Within a unit cell, besides two triangular pores, each hosting a single COR molecule, a rhombic pore is created which hosts two COR molecules (Figure 3a).

As the presence of COR has an impact on the polymorph formation, it is not farfetched that the ratio of COR vs ISA could have an impact on the monolayer composition and architecture as well. This aspect was explored for ISA-OC10. Lowering the COR/ISA ratio gradually reduces the number of COR molecules adsorbed per unit cell. At a COR/ISA molar ratio of 1:10, a hexameric structure where all 6 alkyl chains are interdigitated is observed (Figure 4a). However, the alkyl chain interdigitation does not involve the whole end-to-end distance of adjacent alkyl chains in order that the triangular pore becomes large enough to host a single COR molecule. Finally, lowering the COR/ISA molar ratio to 1:100, COR adsorption only occurs in the hexagonal pores while the triangular pores remain vacant (Figure 4b) and ideal alkyl chain interdigitation is restored. This illustrates the flexibility induced by the non-covalent van der Waals interactions: the ISA network reacts by expanding its pores to accommodate more COR, depending on the specific COR/ISA ratio. This is reflected by the unit cell area which increases from 10.9 nm² (1 COR molecules / unit cell) over 11.4 nm² (3 COR molecules /

unit cell) to 14.0 nm² (5 COR molecules / unit cell) at COR/ISA ratios of 1:100, 1:10 and 1:1 respectively.

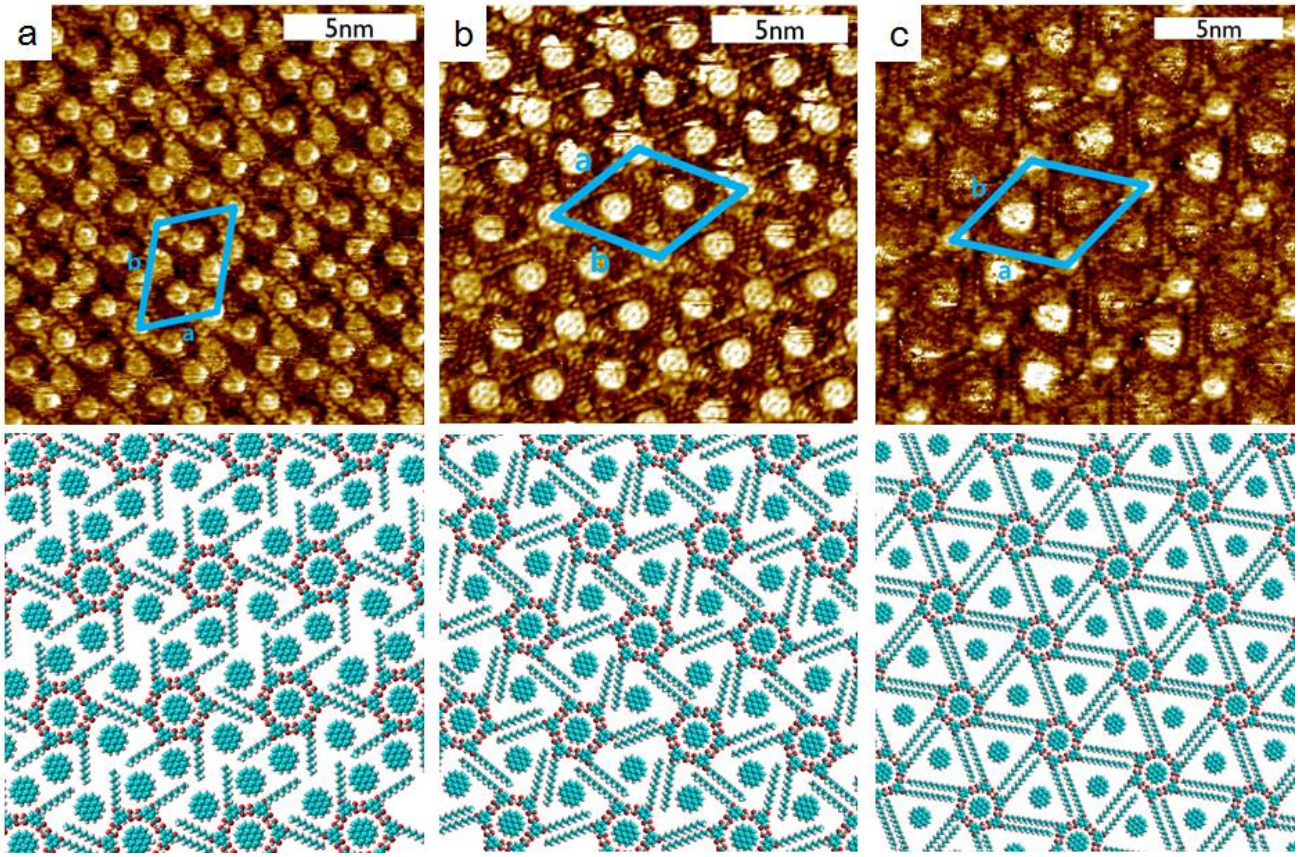

Figure 3: STM images and corresponding tentative models of a mixture of COR and a) ISA-OC10, b) ISA-OC14 and c) ISA-OC18 in a 1:1 ratio (COR/ISA-OC10 1mM/0.98mM, COR/ISA-OC14 3mM/2.65mM, COR/ISA-OC18 0.5mM/0.47mM) Unit cell parameters are a) $\alpha = 68.6 \pm 1.3^{o}$, a = 3.24 ± 0.1 nm , b = 4.64 ± 0.3 nm, b) $\alpha = 59.8 \pm 2.5^{o}$, a = 3.58 ± 0.1 nm , b = 3.66 ± 0.1 nm and c) $\alpha = 59.0 \pm 2.1^{o}$, a = 4.02 ± 0.1 nm , b = 4.18 ± 0.1 nm, respectively.

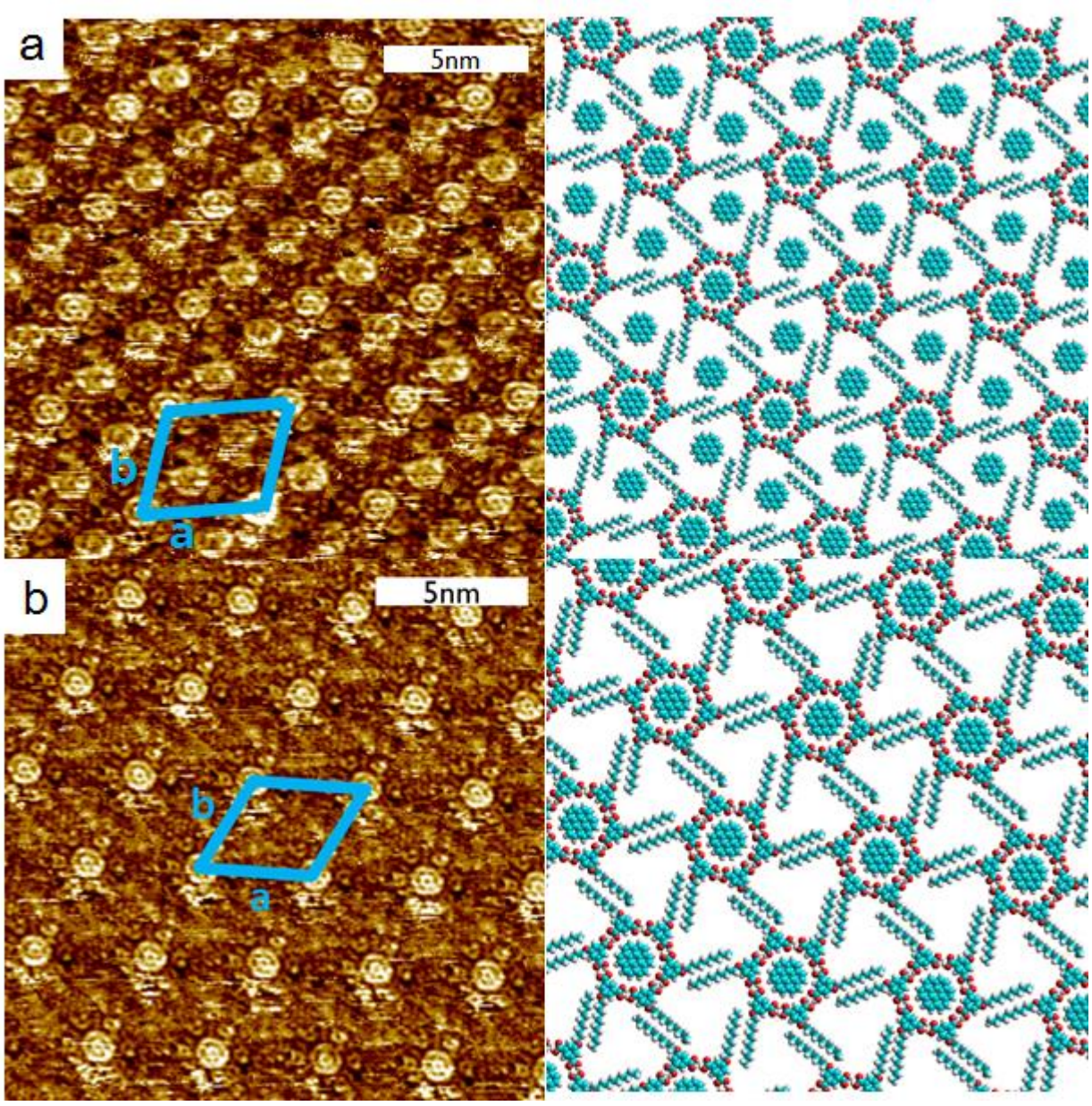

Figure 4: STM images and corresponding tentative molecular models of a premixture of COR and ISA-OC10 at a a) 1:10 ratio (COR: 0.10 mM/ ISA-OC10 0.98 mM, V_{bias} = -0.65 V, I_{set}= 0.12 nA) and a b) 1:100 ratio (COR: 0.01 mM/ ISA-OC10 0.98 mM, V_{bias} = -0.65 V, I_{set}= 0.12 nA) (Unit cell parameters are a) α = 75.6 ± 1.0º, a = 2.94 ± 0.2 nm, b = 4.04 ± 0.1 nm and b) α = 61.7 ± 0.6º, a = 3.67 ± 0.1 nm, b = 3.35 ± 0.1 nm).

Conclusion

We have investigated the self-assembly properties of a series of alkylated isophthalic acid derivatives, which are governed by an interplay of van der Waals interactions and hydrogen bonds. These molecular building blocks can form two distinct polymorphs. It appears that the formation of these polymorphs is very sensitive to external variables. We have shown that it is possible to selectively form a specific network by varying the solute concentration, where high concentration favors a high-density lamellar packing and low concentration favors the formation of low-density porous networks. Moreover, we have demonstrated that a coronene molecule is not only a suitable guest molecule to reside in the pores but may also induce a structural transformation from the lamellar packing to the porous network. Through a combination of these approaches alkylated isophthalic acid derivatives become suitable building blocks to engineer a regular two-dimensional nanoporous network in which the distance between the pores can be tuned at will.

Acknowledgment

This work is supported by the Fund of Scientific Research−Flanders (FWO), KU Leuven (GOA 11/003), Belgian Federal Science Policy Office (IAP-7/05). K.-W.P. and J.H. acknowledge the Basic Science Research Program (2013-026989) through the National Research Foundation (NRF) funded by the Ministry of Science, ICT & Future Planning (MSIP) of Korea. J.A. is a postdoctoral fellow of the Fund of Scientific Research−Flanders (FWO). This research has also received funding from the European Research Council under the European Union's Seventh Framework Programme (FP7/2007-2013)/ERC Grant Agreement No. 340324 as well as from DFG Priority Programme SPP 1459, ERC grant on NANOGRAPH, Graphene Flagship (No. CNECT-ICT-604391), and European Union Projects UPGRADE, GENIUS, and MoQuaS.

(1) Ciesielski, A.; Palma, C.-A.; Bonini, M.; Samorì, P. *Adv. Mater.* **2010**, *22*, 3506.

(2) Mali, K. S.; Adisoejoso, J.; De Cat, I.; Balandina, T.; Ghijsens, E.; Guo, Z.; Li, M.; Sankara Pillai, M.; Vanderlinden, W.; Xu, H.; De Feyter, S. In *Supramolecular Chemistry*; John Wiley & Sons, Ltd: 2012.

(3) Barth, J. V. *Annu Rev Phys Chem* **2007**, *58*, 375.

(4) Nath, K. G.; Ivasenko, O.; MacLeod, J. M.; Miwa, J. A.; Wuest, J. D.; Nanci, A.; Perepichka, D. F.; Rosei, F. *J. Phys. Chem. C* **2007**, *111*, 16996.

(5) Pawin, G.; Wong, K. L.; Kwon, K.-Y.; Bartels, L. *Science* **2006**, *313*, 961.

(6) Kampschulte, L.; Lackinger, M.; Maier, A. K.; Kishore, R. S. K.; Griessl, S.; Schmittel, M.; Heckl, W. M. *J. Phys. Chem. B* **2006**, *110*, 10829.

(7) Stohr, M.; Wahl, M.; Galka, C. H.; Riehm, T.; Jung, T. A.; Gade, L. H. *Angew Chem Int Edit* **2005**, *44*, 7394.

(8) Pawlak, R.; Clair, S.; Oison, V.; Abel, M.; Ourdjini, O.; Zwaneveld, N. A. A.; Gigmes, D.; Bertin, D.; Nony, L.; Porte, L. *Chemphyschem* **2009**, *10*, 1032.

(9) Xue, Y.; Zimmt, M. B. *J. Am. Chem. Soc.* **2012**, *134*, 4513.

(10) Zhang, X.; Chen, T.; Chen, Q.; Deng, G.-J.; Fan, Q.-H.; Wan, L.-J. *Chem. Eur. J.* **2009**, *15*, 9669.

(11) Schull, G.; Douillard, L.; Fiorini-Debuisschert, C.; Charra, F.; Mathevet, F.; Kreher, D.; Attias, A. J. *Adv. Mater.* **2006**, *18*, 2954.

(12) Tahara, K.; Lei, S.; Adisoejoso, J.; De Feyter, S.; Tobe, Y. *Chem. Commun.* **2010**, *46*, 8507.

(13) Adisoejoso, J.; Li, Y.; Liu, J.; Liu, P. N.; Lin, N. *J. Am. Chem. Soc.* **2012**, *134*, 18526.

(14) Stepanow, S.; Lingenfelder, M.; Dmitriev, A.; Spillmann, H.; Delvigne, E.; Lin, N.; Deng, X. B.; Cai, C. Z.; Barth, J. V.; Kern, K. *Nat. Mater.* **2004**, *3*, 229.

(15) Lingenfelder, M. A.; Spillmann, H.; Dmitriev, A.; Stepanow, S.; Lin, N.; Barth, J. V.; Kern, K. *Chem-Eur J* **2004**, *10*, 1913.

(16) Lei, S.; Tahara, K.; De Schryver, F. C.; Van der Auweraer, M.; Tobe, Y.; De Feyter, S. *Angew. Chem. Int. Ed.* **2008**, *47*, 2964.

(17) Kampschulte, L.; Werblowsky, T. L.; Kishore, R. S. K.; Schmittel, M.; Heckl, W. M.; Lackinger, M. *J. Am. Chem. Soc.* **2008**, *130*, 8502.

(18) Tahara, K.; Furukawa, S.; Uji-i, H.; Uchino, T.; Ichikawa, T.; Zhang, J.; Mamdouh, W.; Sonoda, M.; De Schryver, F. C.; De Feyter, S.; Tobe, Y. *J. Am. Chem. Soc.* **2006**, *128*, 16613.

(19) Palma, C.-A.; Bonini, M.; Llanes-Pallas, A.; Breiner, T.; Prato, M.; Bonifazi, D.; Samori, P. *Chem. Commun.* **2008**, 5289.

(20) Ahn, S.; Matzger, A. J. *J. Am. Chem. Soc.* **2010**, *132*, 11364.

(21) Blunt, M. O.; Adisoejoso, J.; Tahara, K.; Katayama, K.; Van der Auweraer, M.; Tobe, Y.; De Feyter, S. *J. Am. Chem. Soc.* **2013**, *135*, 12068.

(22) Adisoejoso, J.; Tahara, K.; Lei, S.; Szabelski, P.; Rżysko, W.; Inukai, K.; Blunt, M. O.; Tobe, Y.; De Feyter, S. *ACS Nano* **2011**, *6*, 897.

(23) Marie, C.; Silly, F.; Tortech, L.; Müllen, K.; Fichou, D. *ACS Nano.* **2010**, *4*, 1288.

(24) Gutzler, R.; Sirtl, T.; Dienstmaier, J. r. F.; Mahata, K.; Heckl, W. M.; Schmittel, M.; Lackinger, M. *J. Am. Chem. Soc.* **2010**, *132*, 5084.

(25) Bellec, A.; Arrigoni, C.; Schull, G.; Douillard, L.; Fiorini-Debuisschert, C.; Mathevet, F.; Kreher, D.; Attias, A.-J.; Charra, F. *J. Chem. Phys.* **2011**, *134*, 124702.

(26) Yang, Y.; Wang, C. *Curr. Opin. Colloid Int.* **2009**, *14*, 135.

(27) Yibao, L.; Zhun, M.; Guicun, Q.; Yanlian, Y.; Qingdao, Z.; Xiaolin, F.; Chen, W.; Wei, H. *J. Phys. Chem. C* **2008**, *112*, 8649.

(28) De Feyter, S.; Gesquière, A.; Klapper, M.; Müllen, K.; De Schryver, F. C. *Nano Lett.* **2003**, *3*, 1485.

(29) Dickerson, P. N.; Hibberd, A. M.; Oncel, N.; Bernasek, S. L. *Langmuir* **2010**, *26*, 18155.

(30) Bernasek, S. L.; Feng, T. *Surf. Sci.* **2007**, *601*, 2284.

(31) Furukawa, S.; Tahara, K.; De Schryver, F. C.; Van der Auweraer, M.; Tobe, Y.; De Feyter, S. *Angew. Chem. Int. Ed.* **2007**, *46*, 2831.

(32) Griessl, S.; Lackinger, M.; Edelwirth, M.; Hietschold, M.; Heckl, W. M. *Single Molecules* **2002**, *3*, 25.

(33) These orientations are observed randomly throughout a series of adjacent lamella, therefore unit cell parameters were not calculated.

(34) Lei, S.; Surin, M.; Tahara, K.; Adisoejoso, J.; Lazzaroni, R.; Tobe, Y.; Feyter, S. D. *Nano Lett.* **2008**, *8*, 2541.

(35) The specific intermolecular interactions between solvent and ISA molecules or mutual solvent molecules at play remains unknown.

(36) The concentration range probed for ISA-OC10 is limited by its solubility

(37) Blunt, M. O.; Russell, J. C.; Champness, N. R.; Beton, P. H. *Chem. Commun.* **2010**, *46*, 7157.

(38) Li, Y.; Ma, Z.; Deng, K.; Lei, S.; Zeng, Q.; Fan, X.; De Feyter, S.; Huang, W.; Wang, C. *Chem. Eur. J.* **2009**, *15*, 5418.

(39) Lackinger, M.; Heckl, W. M. *Langmuir* **2009**, *25*, 11307.